6394 J. Med. Chem. 2009, 52, 6394–6401
DOI: 10.1021/jm901057p

Journal of Medicinal Chemistry Article

Fluoro-pegylated Chalcones as Positron Emission Tomography Probes for in Vivo Imaging of β-Amyloid Plaques in Alzheimer's Disease

Masahiro Ono,*[,†,‡] Rumi Watanabe,[†] Hidekazu Kawashima,[§] Yan Cheng,[‡] Hiroyuki Kimura,[‡] Hiroyuki Watanabe,[†] Mamoru Haratake,[†] Hideo Saji,[‡] and Morio Nakayama*[,†]

[†]*Department of Hygienic Chemistry, Graduate School of Biomedical Sciences, Nagasaki University, 1-14 Bunkyo-machi, Nagasaki 852-8521, Japan,* [‡]*Department of Patho-Functional Bioanalysis, Graduate School of Pharmaceutical Sciences, Kyoto University, Yoshida Shimoadachi-cho, Sakyo-ku, Kyoto 606-8501, Japan, and* [§]*Department of Nuclear Medicine and Diagnostic Imaging, Graduate School of Medicine, Kyoto University, Shogoin Kawahara-cho, Sakyo-ku, Kyoto 606-8507, Japan*

Received July 16, 2009

This paper describes the synthesis and biological evaluation of fluoro-pegylated (FPEG) chalcones for the imaging of β-amyloid (Aβ) plaques in patients with Alzheimer's disease (AD). FPEG chalcone derivatives were prepared by the aldol condensation reaction. In binding experiments conducted in vitro using Aβ(1−42) aggregates, the FPEG chalcone derivatives having a dimethylamino group showed higher K_i values (20−50 nM) than those having a monomethylamino or a primary amine group. When the biodistribution of ^{11}C-labeled FPEG chalcone derivatives having a dimethyamino group was examined in normal mice, all four derivatives were found to display sufficient uptake for imaging Aβ plaques in the brain. ^{18}F-labeled **7c** also showed good uptake by and clearance from the brain, although a slight difference between the ^{11}C and ^{18}F tracers was observed. When the labeling of Aβ plaques was carried out using brain sections of AD model mice and an AD patient, the FPEG chalcone derivative **7c** intensely labeled Aβ plaques. Taken together, the results suggest **7c** to be a useful candidate PET tracer for detecting Aβ plaques in the brain of patients with AD.

Introduction

The formation of β-amyloid (Aβ[a]) plaques is a key neurodegenerative event in Alzheimer's disease (AD).[1,2] Because the imaging of Aβ plaques in vivo may lead to the presymptomatic diagnosis of AD, many radiotracers that bind to Aβ plaques have been developed.[3,4] Preliminary reports of positron emission tomography (PET) suggested that the uptake and retention of 2-(4′-[^{11}C]methylaminophenyl)-6-hydroxybenzothiazole ([^{11}C]PIB, **1**)[5,6] and 4-*N*-[^{11}C]methylamino-4′-hydroxystilbene ([^{11}C]SB-13, **2**)[7,8] differed between the brain of AD patients and those of controls. However, because ^{11}C is a positron-emitting isotope with a $t_{1/2}$ of just 20 min, efforts are being made to develop comparable agents labeled with the isotope ^{18}F ($t_{1/2}$ = 110 min). [^{18}F]-2-(1-(2-(*N*-(2-fluoroethyl)-*N*-methylamino)-naphthalene-6-yl)ethylidene)malononitrile ([^{18}F]FDDNP, **3**)[9,10] and [^{18}F]-4-(*N*-methylamino)-4′-(2-(2-(2-fluoroethoxy)ethoxy)ethoxy)-stilbene ([^{18}F]BAY94−9172, **4**)[11,12] should be useful as tracers for imaging Aβ plaques in the diagnosis of AD. Recent reports suggest that Aβ aggregates possess multiple ligand-binding sites, the density of which differs.[13−15] Therefore, the development of novel probes that bind Aβ aggregates may lead to critical findings regarding the pathology of AD.

Recently, in a search for novel Aβ-imaging probes, we found that radioiodinated flavone,[16,17] chalcone,[18,19] and aurone[20,21] derivatives, which are categorized as flavonoids, showed excellent characteristics such as high affinity for Aβ aggregates and good uptake into and rapid clearance from the brain. The chalcone structure in particular is considered to be a useful core in the development of new Aβ-imaging probes because it can be formed by a one-pot condensation reaction. In addition, because chalcone derivatives show different characteristics of binding to Aβ aggregates from Congo Red and thioflavin T, they are expected to provide new information from in vivo imaging in AD brains.

In the present study, we designed and synthesized fluorinated chalcone derivatives for the purpose of developing ^{18}F-labeled probes for PET-based imaging of Aβ plaques. The formation of bioconjugates based on pegylation-fluorination resulting in fluoro-pegylated (FPEG) molecules is effective for some core structures of Aβ-imaging probes.[22] We have adopted a novel approach, adding a short PEG (n = 1−3) to the chalcone backbone and capping the end of the ethylene glycol chain with a fluorine atom. Indeed, the most promising ^{18}F-labeled agent **4** possesses PEG (n = 3) in the stilbene backbone. This tracer showed strong affinity (K_i = 6.7 nM) for Aβ plaques, high uptake (7.77%ID/g at 2 min postinjection), and rapid clearance from the mouse brain

*To whom correspondence should be addressed. For M.O.: phone, +81-75-753-4608; fax, +81-75-753-4568; E-mail, ono@pharm.kyoto-u.ac.jp. For M.N.: phone, +81-95-819-2441; fax, +81-95-819-2441; E-mail: morio@nagasaki-u.ac.jp.

[a] Abbreviations: Aβ, β-amyloid; AD, Alzheimer's disease; PET, positron emission tomography; PIB, 2-(4′-methyaminophenyl)-6-hydroxybenzothiazole; SB-13, 4-*N*-methylamino-4′-hydroxystilbene; FDDNP, 2-(1-(2-(*N*-(2-fluoroethyl)-*N*-methylamino)naphthalene-6-yl)ethylidene)-malononitrile; BAY94-9174, 4-(*N*-methylamino)-4′-(2-(2-(2-fluoroethoxy)ethoxy)ethoxy)-stilbene; DMIC, 4-dimethylamino-4′-iodo-chalcone; IMPY, 6-iodo-2-(4′-dimethylamino)phenyl-imidazo[1,2-*a*]pyridine; FPEG, fluoro-pegylated; DAST, diethylamino sulfur trifluoride; DME, 1,2-dimethoxyethane; MEK, methyl ethyl ketone; [^{11}C]methyl triflate, [^{11}C]MeOTf; DAB, 3,3′-diaminobenzidine.

 Published on Web 09/16/2009

Scheme 1

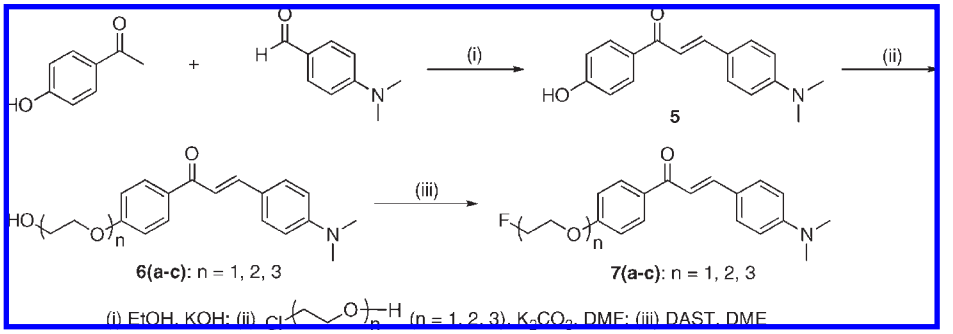

Scheme 2

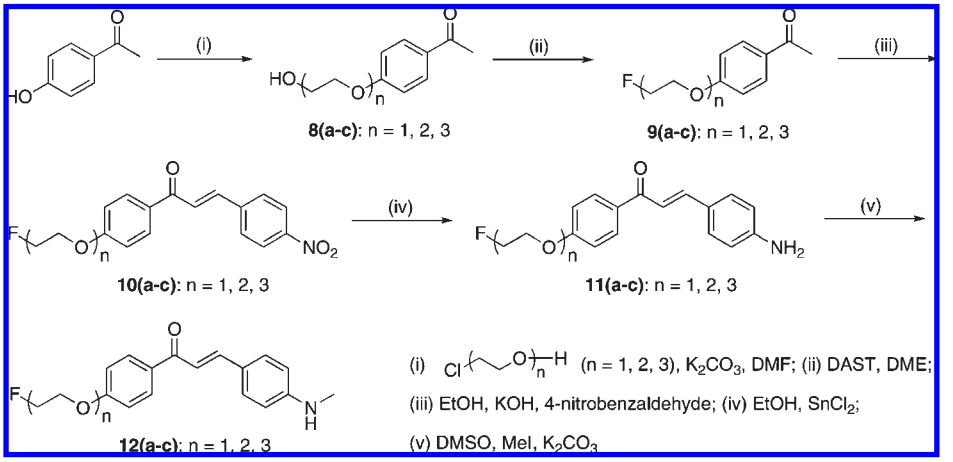

Scheme 3[a]

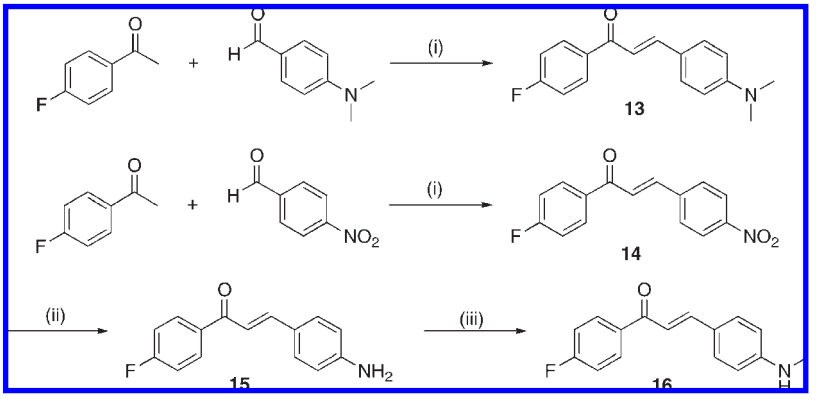

[a] (i) EtOH, KOH; (ii) EtOH, $SnCl_2$; (iii) DMSO, MeI, K_2CO_3.

(1.61%ID/g at 60 min postinjection).[12] We adopted the biological data for **4** as criteria to develop novel Aβ-imaging agents. In this study, we synthesized 12 fluorinated chalcones and evaluated their biological potential as Aβ-imaging agents by testing their affinity for Aβ aggregates and Aβ plaques in sections of brain tissue from AD model mice and an AD patient and their uptake by and clearance from the brain in biodistribution experiments using normal mice.

Results and Discussion

The synthesis of the FPEG chalcone derivatives is outlined in Schemes 1, 2, and 3. The most useful way to prepare chalcones is the condensation of acetophenones with ben zaldehydes. Using this process, 4-hydroxyacetophenone or 4-fluoroacetophenone was reacted with 4-dimethylaldehyde to form 4′-hydroxy-4-dimethylamino-chalcone **5** and 4′-fluoro-4-dimethylamino-chalcone **13** in yields of 84.0 and 41.6%, respectively. Compounds **10**(**a**−**c**) were synthesized by an aldol reaction between FPEG acetophenone **9**(**a**−**c**) and 4-nitrobenzaldehyde. Fluorination of **6**(**a**−**c**) and **8**(**a**−**c**) to prepare **7**(**a**−**c**) and **9**(**a**−**c**) was done using diethylamino sulfur trifluoride (DAST) after introducing three oligoethylene glycol molecules into the phenolic OH of **5** and **9**(**a**−**c**). The amino derivatives **11**(**a**−**c**) and **15** were readily prepared from **10**(**a**−**c**) and **14** by reduction with $SnCl_2$. Conversion of **11**(**a**−**c**) and **15** to the monomethylamino derivatives **12**(**a**−**c**) and **16** was achieved by methylation with CH_3I under alkaline conditions. Preparation of ^{11}C-labeled compounds was done as in Scheme 4. ^{11}C-labeled chalcones

Scheme 4

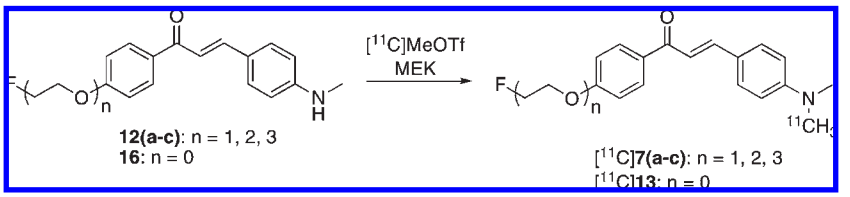

Scheme 5

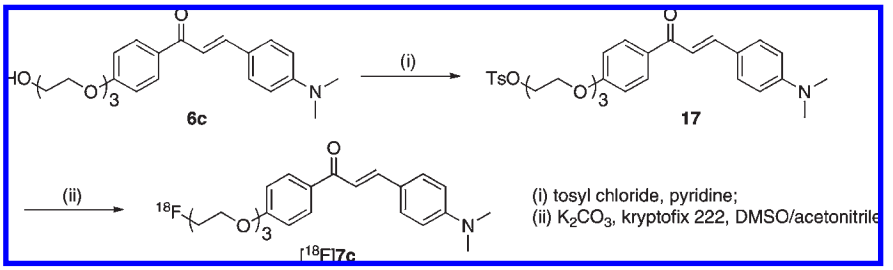

Table 1. Chemical Structures and Inhibition Constants of Fluorinated Chalcone Derivatives

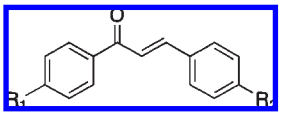

compd	R_1	R_2	K_i (nM)[a]
7a	FCH_2CH_2O	$N(CH_3)_2$	45.7 ± 7.1
7b	$F(CH_2CH_2O)_2$	$N(CH_3)_2$	20.0 ± 2.5
7c	$F(CH_2CH_2O)_3$	$N(CH_3)_2$	38.9 ± 4.2
11a	FCH_2CH_2O	NH_2	678.9 ± 21.7
11b	$F(CH_2CH_2O)_2$	NH_2	1048.0 ± 114.3
11c	$F(CH_2CH_2O)_3$	NH_2	790.0 ± 132.1
12a	FCH_2CH_2O	$NHCH_3$	197.1 ± 58.8
12b	$F(CH_2CH_2O)_2$	$NHCH_3$	216.4 ± 13.8
12c	$F(CH_2CH_2O)_3$	$NHCH_3$	470.9 ± 100.4
13	F	$N(CH_3)_2$	49.8 ± 6.2
15	F	NH_2	663.0 ± 88.3
16	F	$NHCH_3$	234.2 ± 44.0
DMIC	I	$N(CH_3)_2$	13.1 ± 3.0
IMPY			28.0 ± 4.1

[a] Inhibition constants (K_i, nM) of compounds for the binding of [^{125}I]DMIC to Aβ(1−42) aggregates. Values are the mean ± standard error of the mean for 4−9 independent experiments.

were readily synthesized from their *N*-normethyl precursors, **12**(**a**−**c**) and **16**, and [^{11}C]methyl triflate ([^{11}C]-MeOTf). Radiochemical yields of the final product were 28−35%, decay corrected to end of bombardment. Radiochemical purity was >99% with a specific activity of 22−28 GBq/μmol. The identity of [^{11}C]**7a**, [^{11}C]**7b**, [^{11}C]**7c**, and [^{11}C]**13** was confirmed by a comparison of HPLC retention times with the nonradioactive compounds (**7a**, **7b**, **7c**, and **13**). ^{18}F labeling of **7c** was performed on a tosyl precursor **17** undergoing a nucleophilic displacement reaction with the fluoride anion (Scheme 5). Radiolabeling with ^{18}F was successfully performed on the precursor to generate [^{18}F]**7c** with a radiochemical yield of 45% and radiochemical purity >99%. The identity of [^{18}F]**7c** was verified by a comparison of retention time with the nonradioactive compound. The specific activity of [^{18}F]**7c** was estimated to be 35 GBq/mmol at the end of synthesis.

Table 2. Biodistribution of Radioactivity after Injection of [^{11}C]**7a**, [^{11}C]**7b**, [^{11}C]**7c**, and [^{11}C]**13** in Normal Mice[a]

organ	2 min	10 min	30 min	60 min
		[^{11}C]**7a**		
blood	3.65 ± 0.37	2.73 ± 0.28	2.12 ± 0.18	2.22 ± 0.25
brain	6.01 ± 0.61	3.24 ± 0.39	2.57 ± 0.26	2.26 ± 0.41
		[^{11}C]**7b**		
blood	3.48 ± 0.56	2.28 ± 0.84	2.54 ± 0.96	1.44 ± 0.36
brain	4.73 ± 0.47	2.23 ± 0.18	1.14 ± 0.12	1.00 ± 0.19
		[^{11}C]**7c**		
blood	2.44 ± 0.25	1.52 ± 0.42	1.01 ± 0.15	0.68 ± 0.10
brain	4.31 ± 0.33	1.38 ± 0.16	0.64 ± 0.07	0.35 ± 0.03
		[^{11}C]**13**		
blood	2.61 ± 0.35	1.60 ± 0.25	0.39 ± 0.05	1.40 ± 0.20
brain	3.68 ± 0.35	1.53 ± 0.14	1.04 ± 0.15	1.04 ± 0.20

[a] Expressed as % of injected dose per gram. Each value represents the mean ± SD for 4−5 mice.

Table 3. Biodistribution of Radioactivity after Injection of [^{18}F]**7c** in Normal Mice[a]

organ	2 min	10 min	30 min	60 min
blood	2.09 ± 0.40	1.94 ± 0.18	2.35 ± 0.33	1.87 ± 0.26
brain	3.48 ± 0.47	1.52 ± 0.03	1.08 ± 0.09	1.07 ± 0.17
bone	1.80 ± 0.31	1.76 ± 0.15	2.98 ± 0.49	3.58 ± 0.41

[a] Expressed as % of injected dose per gram. Each value represents the mean ± SD for 4−5 mice.

Experiments in vitro to evaluate the affinity of the FPEG chalcones for Aβ aggregates were carried out in solutions of Aβ aggregates with [^{125}I]4-dimethylamino-4′-iodo-chalcone ([^{125}I]DMIC)[18] as the ligand (Table 1). The K_i values suggested that the binding to Aβ(1−42) aggregates was affected by substitution at the amino group at position 4 in the chalcone structure, not by the length of PEG introduced into the chalcone backbone. The fluorinated chalcones had binding affinity for Aβ(1−42) aggregates in the following order: the dimethyamino derivatives (**7a**, **7b**, **7c**, and **13**) > the monomethylamino derivatives (**12a**, **12b**, **12c**, and **16**) > the primary amino derivatives (**11a**, **11b**, **11c**, and **15**). The result of the binding experiments is consistent with that of previous reports.[16,19] In addition, the affinity of the dimethylamino

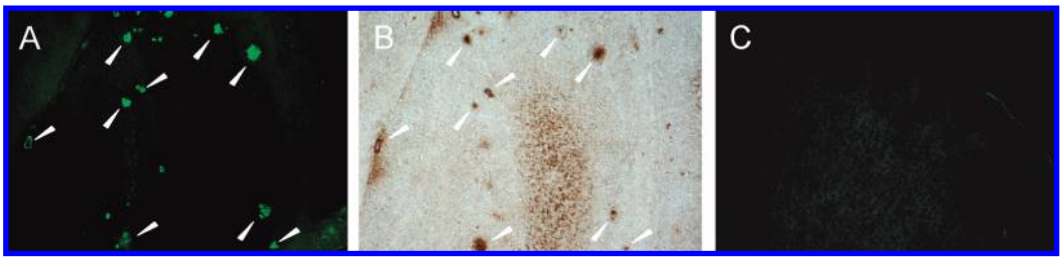

Figure 1. Neuropathological staining of 10 μm sections of a Tg2576 mouse brain (A and B) and aged normal brain (C). Fluorescent staining of compound **7c** in the Tg2576 mouse brain (A). Aβ immunostaining with antibody BC05 in the adjacent section (B). Fluorescent staining of compound **7c** in the age-matched control mouse brain (C).

derivatives was in the same range as that of the known compound, 6-iodo-2-(4′-dimethylamino)phenyl-imidazo[1,2-*a*]pyridine (IMPY), which is commonly used for inhibition assays.[22−25] We selected the dimethylamino derivatives (**7a**, **7b**, **7c**, and **13**), which showed the greatest affinity, for additional studies.

To evaluate brain uptake of the FPEG chalcones, biodistribution experiments were performed in normal mice with four ^{11}C-labeled FPEG chalcones ([^{11}C]**7a**, [^{11}C]**7b**, [^{11}C]**7c**, and [^{11}C]**13**) (Table 2). Because normal mice were used for the biodistribution experiments, no Aβ plaques were expected in the young mice; therefore the washout of probes from the brain should be rapid to obtain a higher signal-to-noise ratio earlier in the AD brain. Radioactivity after injection of the ^{11}C-labeled FPEG chalcones penetrated the blood−brain barrier, showing excellent uptake ranging from 3.7 to 6.0% ID/g brain at 2 min postinjection, a level sufficient for imaging Aβ plaques in the brain. In addition, they displayed good clearance from the normal brain with 2.3, 1.0, 0.35, and 1.0% ID/g at 60 min postinjection for [^{11}C]**7a**, [^{11}C]**7b**, [^{11}C]**7c**, and [^{11}C]**13**, respectively. These values were equal to 37.6, 21.1, 8.1, and 28.3% of the initial uptake peak for [^{11}C]**7a**, [^{11}C]**7b**, [^{11}C]**7c**, and [^{11}C]**13**, respectively. Compound **7c** with the fastest washout from the brain was labeled with ^{18}F and evaluated for its biodistribution in normal mice (Table 3). [^{18}F]**7c** displayed high uptake (3.48%ID/g) at 2 min postinjection, a level sufficient for imaging like [^{11}C]**7c**, and was cleared over the subsequent 10, 30, and 60 min. The radioactivity in the brain at 60 min postinjection was 1.07%ID/g, indicating that this [^{18}F]**7c** has favorable pharmacokinetics in the brain. Although we consider that a slight difference of the radioactivity pharmacokinetics between [^{11}C]**7c** and [^{18}F]**7c** could be attributable to the different physicochemical characteristics of their radiometabolites produced in the brain, the reason for this difference has remained unclear. Bone uptake at 60 min was measurable (3.58%ID/g), suggesting defluorination in vivo. Bone uptake has been observed for other ^{18}F tracers.[12,22−24] However, previous reports suggested that free fluoride was not taken up by brain tissue; therefore, the interference from free fluoride may be relatively low for brain imaging. A previous paper regarding the most promising ^{18}F-labeled agent **4** reported that it showed high uptake (7.77% ID/g at 2 min postinjection) and rapid clearance from the brain (1.61%ID/g at 60 min postinjection) with little accumulation in bone (1.77%ID/g at 60 min postinjection) in biodistribution experiments using normal mice.[12] The pharmacokinetics of **4** appear superior to that of [^{18}F]**7c**, but the good biological results obtained with [^{18}F]**7c** suggest that further investigation is warranted.

To investigate the ability of the fluorinated chalcones to bind to Aβ plaques in the AD model, fluorescent staining of sections of mouse brain were carried out with compound **7c** (Figure 1). We used Tg2576 transgenic mice as an animal model of Aβ plaque deposition, which express human APP695 with the K670N, M671L Swedish double mutation.[26] By 11−13 months of age, Tg2576 mice show prominent Aβ deposition in the cingulated cortex, entorhinal cortex, dentate gyrus, and CA1 hippocampal subfield and have been frequently used for the evaluation of specific binding of Aβ plaques in in vitro and in vivo experiments.[12,24,27−31] Many Aβ plaques were clearly stained with **7c**, as reflected by the affinity for the aggregates of synthetic Aβ(1−42) in in vitro competition assays (Figure 1A). The labeling pattern was consistent with that observed after immunohistochemical labeling by BC05, a specific antibody for Aβ (Figure 1B), while wild-type mouse brain displayed no significant accumulation of **7c** (Figure 1C). The results indicated that **7c** binds specifically to Aβ plaques in Tg2576 mice brain. A previous report suggested the configuration/folding of Aβ plaques in Tg2576 mice to be different from the tertiary/quaternary structure of Aβ plaques in AD brains.[30,32] In addition, the studies reported with **1** further indicate that the binding of **1** reflects the amount of Aβ plaques in human AD brain but not in Tg2576 mouse brain, and the detectability of Aβ plaques by **1** is dependent on the accumulation of specific Aβ subtypes.[28,29] Therefore, we considered that it should be essential to evaluate the binding affinity for Aβ plaques in human AD brains because our goal is to develop clinically useful probes for in vivo imaging of Aβ plaques in humans.

Next, we investigated the binding affinity of [^{18}F]**7c** for Aβ plaques by in vitro autoradiography in a human AD brain section (Figure 2A). The autoradiographic image of [^{18}F]**7c** showed high levels of radioactivity in some specific areas of the brain section. Furthermore, we confirmed that the hot spots of [^{18}F]**7c** in an AD brain section corresponded with those of in vitro thioflavin-S staining in the same brain section (Figure 2B). In contrast, no significant accumulation of [^{18}F]**7c** was observed in the region without Aβ plaques (Figure 2C). The results demonstrate the feasibility of using [^{18}F]**7c** as a probe for detecting Aβ plaques in the brain of AD patients with PET.

In conclusion, we reported novel FPEG chalcone derivatives, containing an end-capped fluoropolyethylene glycol as in vivo PET imaging agents for Aβ plaques in the brain. The FPEG chalcones with a dimethylamino group displayed greater affinity for synthetic Aβ aggregates than did the monomethylamino and primary amino derivatives. In biodistribution experiments using normal mice, ^{11}C-labeled FPEG chalcones displayed sufficient uptake for the imaging of Aβ plaques in the brain. [^{11}C]**7c** showed the fastest clearance from the brain, probably related to a low nonspecific binding. [^{18}F]**7c** also displayed high uptake in and good clearance from

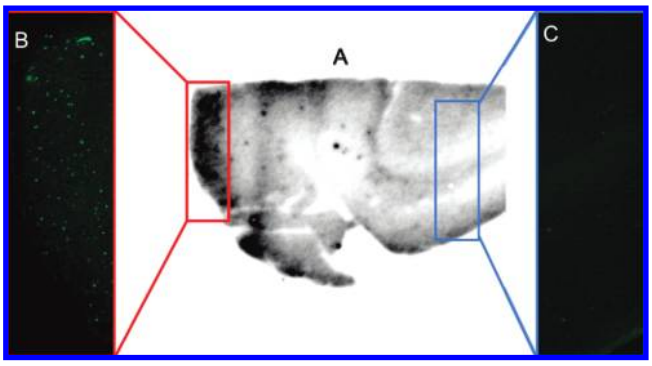

Figure 2. In vitro autoradiography of [^{18}F]**7c** using the human AD brain section (A). Aβ plaques were confirmed by in vitro staining of the same section with thioflavin-S (B and C).

the brain, although a slight difference was observed between the ^{11}C and ^{18}F tracers. When the labeling of plaques in vitro was carried out using sections of brain tissue from an animal model of AD and an AD patient, compound **7c** intensely labeled Aβ plaques existing in both brains. Taken together, the results suggest the novel FPEG chalcone **7c** to be potentially useful for imaging Aβ plaques in the brain using PET.

Experimental Section

General. All reagents were obtained commercially and used without further purification unless otherwise indicated. ^{1}H NMR spectra were obtained on a Varian Gemini 300 spectrometer with TMS as an internal standard. Coupling constants are reported in hertz. Multiplicity was defined by s (singlet), d (doublet), t (triplet) and m (multiplet). Mass spectra were obtained on a JEOL IMS-DX instrument. HPLC analysis was performed on a Shimadzu HPLC system (a LC-10AT pump with a SPD-10A UV detector, $\lambda = 254$ nm) using a Cosmosil C_{18} column (Nakalai Tesque, 5C_{18}-AR-II, 4.6 mm × 150 mm) using acetonitrile/water (50/50) as mobile phase at a flow rate of 1.0 mL/min. All key compounds were proven by this method to show ≥95% purity.

Chemistry. (*E*)-3-(4-(Dimethylamino)phenyl)-1-(4-hydroxyphenyl)-2-propen-1-one (5). 4-Hydroxyacetophenone (1.36 g, 10 mmol) and 4-dimethylaminobenzaldehyde (1.86 g, 10.0 mmol were dissolved in EtOH (15 mL). A 30 mL aliquot of a 10% aqueous KOH solution was then slowly added dropwise to the reaction mixture. The mixture was stirred for 24 h at 100 °C and then extracted with ethyl acetate. After the organic layers were combined and dried over Na_2SO_4, evaporation of the solvent afforded 1.50 g of **5** (84.0%). ^{1}H NMR (CD_3OD) δ: 3.04 (s, 6H), 6.76 (d, $J = 8.7$ Hz, 2H), 6.88 (d, $J = 8.7$ Hz, 2H), 7.50 (d, $J = 15.3$ Hz, 1H), 7.59 (d, $J = 9.0$ Hz, 2H), 7.72 (d, $J = 15.3$ Hz, 1H), 7.98 (d, $J = 8.7$ Hz, 2H). ^{1}H NMR (DMSO-d_6) δ: 2.99 (s, 6H), 6.74 (d, $J = 8.7$ Hz, 2H), 6.88 (d, $J = 8.4$ Hz, 2H), 7.62 (s, 2H), 7.68 (d, $J = 8.7$ Hz, 2H), 8.03 (d, $J = 8.7$ Hz, 2H), 10.30 (s, 1H). EI-MS: m/z 267 (M^+).

(*E*)-3-(4-(Dimethylamino)phenyl)-1-(4-(2-hydroxyethoxy)phenyl)-2-propen-1-one (6a). To a solution of **5** (500 mg, 1.87 mmol and ethylene chlorohydrin (125 μL, 1.87 mmol) in DMSO (5 mL) was added anhydrous K_2CO_3 (775 mg, 5.61 mmol). The reaction mixture was stirred for 18 h at 100 °C and then poured into water and extracted with chloroform. The organic layers were combined and dried over Na_2SO_4. Evaporation of the solvent afforded a residue, which was purified by silica gel chromatography (hexane: ethyl acetate = 1:1) to give 422 mg of **6a** (72.7%). ^{1}H NMR ($CDCl_3$) δ: 3.04 (s, 6H), 4.00−4.01 (m, 2H), 4.17 (t, $J = 4.8$ Hz, 2H), 6.69 (d, $J = 9.0$ Hz, 2H), 6.99 (d, $J = 6.9$ Hz, 2H), 7.35 (d, $J = 15.3$ Hz, 1H), 7.55 (d, $J = 9.0$ Hz, 2H), 7.79 (d, $J = 15.3$ Hz, 1H), 8.02 (d, $J = 9.3$ Hz, 2H).

(*E*)-3-(4-(Dimethylamino)phenyl)-1-(4-(2-(hydroxyethoxy)ethoxy)-phenyl)-2-propen-1-one (6b). The reaction described above to prepare **6a** was used, and **6b** was obtained from **5** and ethylene glycol mono-2-chloroethyl ether. ^{1}H NMR ($CDCl_3$) δ: 3.05 (s, 6H), 3.69 (t, $J = 4.8$ Hz, 2H), 3.78 (s, 2H), 3.91 (t, $J = 4.8$ Hz, 2H), 4.23 (t, $J = 4.8$ Hz, 2H), 6.70 (d, $J = 9.0$ Hz, 2H), 6.99 (d, $J = 9.0$ Hz, 2H), 7.35 (d, $J = 15.3$ Hz, 1H), 7.55 (d, $J = 8.7$ Hz, 2H), 7.79 (d, $J = 15.6$ Hz, 1H), 8.02 (d, $J = 9.0$ Hz, 2H).

(*E*)-3-(4-(Dimethylamino)phenyl)-1-(4-(2-((hydroxyethoxy)ethoxy)-ethoxy)phenyl)-2-propen-1-one (6c). The reaction described above to prepare **6a** was used, and 429 mg of **6c** was obtained in a yield of 82.6% from **5** and 2-[2-(2-chloroethoxy)-ethoxy]ethanol. ^{1}H NMR ($CDCl_3$) δ: 3.04 (s, 6H), 3.62 (t, $J = 5.1$ Hz, 2H), 3.73−3.75 (m, 6H), 3.90 (t, $J = 4.8$ Hz, 2H), 4.22 (t, $J = 4.8$ Hz, 2H), 6.70 (d, $J = 9.0$ Hz, 2H), 6.99 (d, $J = 8.7$ Hz, 2H), 7.35 (d, $J = 15.3$ Hz, 1H), 7.55 (d, $J = 9.0$ Hz, 2H), 7.78 (d, $J = 15.3$ Hz, 1H), 8.02 (d, $J = 9.0$ Hz, 2H).

(*E*)-3-(4-(Dimethylamino)phenyl)-1-(4-(2-fluoroethoxy)phenyl)-2-propen-1-one (7a). To a solution of **6a** (100 mg, 0.32 mmol in 1,2-dimethoxyethane (DME) (5 mL) was added DAST (85 μL, 0.64 mmol) in a dry ice−acetone bath. The reaction mixture was stirred for 1 h at room temperature and then poured into a saturated $NaHSO_3$ solution and extracted with chloroform. After the organic phase was separated, dried over Na_2SO_4, and filtered, and the residue was purified by preparative TLC (hexane:ethyl acetate = 3:1) to give 39 mg of **7a** (38.9%). ^{1}H NMR ($CDCl_3$) δ: 3.09 (s, 6H), 4.30 (d, t, $J_1 = 27.6$ Hz, $J_2 = 4.2$ Hz, 2H), 4.79 (d, t, $J_1 = 47.4$ Hz, $J_2 = 4.2$ Hz, 2H), 6.70 (d, $J = 8.7$ Hz, 2H), 7.00 (d, $J = 9.0$ Hz, 2H), 7.35 (d, $J = 15.6$ Hz, 1H), 7.55 (d, $J = 9.0$ Hz, 2H), 7.79 (d, $J = 15.3$ Hz, 1H), 8.03 (d, $J = 9.0$ Hz, 2H). EI-MS: m/z 313 (M^+).

(*E*)-3-(4-(Dimethylamino)phenyl)-1-(4-(2-(fluoroethoxy)ethoxy)-phenyl)-2-propen-1-one (7b). The reaction described above to prepare **7a** was used, and 28 mg of **7b** was obtained in a yield of 28.0% from **6b**. ^{1}H NMR ($CDCl_3$) δ: 3.04 (s, 6H), 3.77−3.94 (m, 4H), 4.21−4.24 (m, 3H), 4.61 (d, t, $J_1 = 47.4$ Hz, $J_2 = 4.2$ Hz 1H), 6.69 (d, $J = 9.3$ Hz, 2H), 6.99 (d, $J = 8.7$ Hz, 2H), 7.35 (d, $J = 15.3$ Hz, 2H), 7.55 (d, $J = 9.0$ Hz, 2H), 7.78 (d, $J = 15.6$ Hz, 2H), 8.02 (d, $J = 9.0$ Hz, 2H). EI-MS: m/z 357 (M^+).

(*E*)-3-(4-(Dimethylamino)phenyl)-1-(4-(2-((fluoroethoxy)ethoxy)-ethoxy)phenyl)-2-propen-1-one (7c). The reaction described above to prepare **7a** was used, and 29 mg of **7c** was obtained in a yield of 14.4% from **6c** and 2-[2-(2-chloroethoxy)ethoxy]ethanol. ^{1}H NMR ($CDCl_3$) δ: 3.04 (s, 6H), 3.73−3.81 (m, 6H), 3.90 (t, $J = 5.1$ Hz, 2H), 4.21 (t, $J = 5.1$ Hz, 2H), 4.49 (t, $J = 4.5$ Hz, 1H), 4.65 (t, $J = 4.5$ Hz, 1H), 6.70 (d, $J = 8.7$ Hz, 2H), 6.98 (d, $J = 9.0$ Hz, 2H), 7.35 (d, $J = 15.3$ Hz, 1H), 7.55 (d, $J = 8.7$ Hz, 2H), 7.78 (d, $J = 15.3$ Hz, 1H), 8.02 (d, $J = 9.0$ Hz, 2H). EI-MS: m/z 401 (M^+).

1-(4-(2-Hydroxyethoxy)phenyl)ethanone (8a). The reaction described above to prepare **6a** was used, and 1.79 g of **8a** was obtained in a yield of 99.4% from 4-hydroxyacetophenone and ethylene chlorohydrin. ^{1}H NMR ($CDCl_3$) δ: 2.75 (s, 3H), 4.20 (s, 2H), 4.35 (t, $J = 5.1$ Hz, 2H), 7.15 (d, $J = 9.0$ Hz, 2H), 8.13 (d, $J = 9.0$ Hz, 2H).

1-(4-(2-(2-Hydroxyethoxy)ethoxy)phenyl)ethanone (8b). The reaction described above to prepare **6b** was used, and **8b** was obtained from 4-hydroxyacetophenone and ethylene glycol mono-2-chloroethyl ether. ^{1}H NMR ($CDCl_3$) δ: 2.56 (s, 3H), 3.68 (t, $J = 4.8$ Hz 2H), 3.75−3.79 (m, 2H) 3.90 (t, $J = 5.1$ Hz, 2H), 4.21 (t, $J = 4.8$ Hz, 2H), 6.96 (d, $J = 8.7$ Hz, 2H), 7.94 (d, $J = 8.7$ Hz, 2H).

1-(4-(2-(2-(2-Hydroxyethoxy)ethoxy)ethoxy)phenyl)ethanone (8c). The reaction described above to prepare **6a** was used, and **8c** was obtained from 4-hydroxyacetophenone and 2-[2-(chloroethoxy)ethoxy]ethanol. ^{1}H NMR ($CDCl_3$) δ: 2.50 (s, 3H), 3.72−3.83 (m, 6H), 3.92 (t, $J = 4.5$ Hz, 2H), 4.22 (t, $J = 5.1$ Hz, 2H), 4.49 (t, $J = 4.2$ Hz, 1H), 4.61 (t, $J = 4.2$ Hz, 1H), 6.86 (d, $J = 8.7$ Hz, 2H), 7.80 (d, $J = 8.7$ Hz, 2H).

1-(4-(2-Fluoroethoxy)phenyl)ethanone (9a). The reaction described above to prepare **7a** was used, and 1.02 g of **9a** was obtained

in a yield of 63.3% from **8a** and DAST. ^{1}H NMR ($CDCl_3$) δ: 4.24 (d, t, J_1 = 28.2 Hz, J_2 = 4.2 Hz, 2H), 4.75 (d, t, J_1 = 47.1 Hz, J_2 = 3.9 Hz, 2H), 6.92 (d, J = 9.0 Hz, 2H), 7.89 (d, J = 9.3 Hz, 2H).

1-(4-(2-(2-Fluoroethoxy)ethoxy)phenyl)ethanone (9b). The reaction described above to prepare **7b** was used, and **9b** was obtained from **9a** and DAST. ^{1}H NMR ($CDCl_3$) δ: 2.56 (s, 3H), 3.78 (t, J = 3.3 Hz, 1H), 3.86−3.94 (m, 3H), 4.22 (t, J = 5.1 Hz, 2H), 4.51 (t, J = 3.0 Hz, 1H), 4.67 (t, J = 3.0.Hz, 1H), 6.96 (d, J = 8.7 Hz, 2H), 7.93 (d, J = 8.7 Hz, 2H). EI-MS: m/z 226 (M^+).

1-(4-(2-(2-(2-Fluoroethoxy)ethoxy)ethoxy)phenyl)ethanone (9c). The reaction described above to prepare **7c** was used, and 543 mg of **9c** was obtained from **8c** and DAST. ^{1}H NMR ($CDCl_3$) δ: 2.56 (s, 3H), 3.69−3.81 (m, 6H), 3.90 (t, J = 4.5 Hz, 2H), 4.21 (t, J = 5.1 Hz, 2H), 4.49 (t, J = 4.2 Hz, 1H), 4.65 (t, J = 4.2 Hz, 1H), 6.95 (d, J = 9.3 Hz, 2H), 7.92 (d, J = 9.0 Hz, 2H). EI-MS: m/z 270 (M^+).

(*E*)-1-(4-(2-Fluoroethoxy)phenyl)-3-(4-nitrophenyl)-2-propen-1-one (10a). The reaction described above to prepare **5** was used, and 856 mg of **10a** was obtained in a yield of 56.6% from **9a** and 4-nitrobenzaldehyde. ^{1}H NMR ($CDCl_3$) δ: 4.32 (d, t, J_1 = 27.6 Hz, J_2 = 4.2 Hz, 2H), 4.81 (d, t, J_1 = 47.4 Hz, J_2 = 4.2 Hz, 2H), 7.04 (d, J = 8.7 Hz, 2H), 7.65 (d, J = 15.6 Hz, 1H), 7.79 (d, J = 8.7 Hz, 2H), 7.82 (d, J = 12.6 Hz, 1H), 8.06 (d, J = 9.0 Hz, 2H), 8.28 (d, J = 8.7 Hz, 2H).

(*E*)-1-(4-(2-(Fluoroethoxy)ethoxy)phenyl)-3-(4-nitrophenyl)-2-propen-1-one (10b). The reaction described above to prepare **5** was used, and 128 mg of **10b** was obtained from **9b** and 4-nitrobenzaldehyde. ^{1}H NMR ($CDCl_3$) δ: 3.79 (t, J = 4.2 Hz, 1H), 3.88−4.27 (m, 3H), 4.8 (t, J = 4.8 Hz, 2H), 4.53 (t, J = 4.2 Hz, 1H), 4.69 (t, J = 4.2 Hz, 1H), 7.03 (d, J = 8.7 Hz, 2H), 7.66 (d, J = 15.6 Hz, 1H), 7.79 (d, J = 9.0 Hz, 2H), 7.81 (d, J = 15.6 Hz, 1H), 8.05 (d, J = 8.7 Hz, 2H), 8.28 (d, J = 9.0 Hz, 2H).

(*E*)-1-(4-(2-((Fluoroethoxy)ethoxy)ethoxy)phenyl)-3-(4-nitrophenyl)-2-propen-1-one (10c). The reaction described above to prepare **5** was used, and 649 mg of **10c** was obtained from **9c**. ^{1}H NMR ($CDCl_3$) δ: 3.71−3.82 (m, 6H), 3.92 (t, J = 4.5 Hz, 2H), 4.24 (t, J = 4.8 Hz, 2H), 4.50 (t, J = 4.2 Hz, 1H), 4.66 (t, J = 4.5 Hz, 1H), 7.03 (d, J = 9.3 Hz, 2H), 7.66 (d, J = 15.6 Hz, 1H), 7.79 (d, J = 9.0 Hz, 2H), 7.81 (d, J = 15.6 Hz, 1H), 8.05 (d, J = 9.3 Hz, 2H), 8.28 (d, J = 8.7 Hz, 2H).

(*E*)-3-(4-Aminophenyl)-1-(4-(2-fluoroethoxy)phenyl)-2-propen-1-one (11a). A mixture of **10a** (856 mg, 2.7 mmol), $SnCl_2$ (2.55 g, 13.5 mmol), and EtOH (10 mL) was stirred at 100 °C for 2 h. After the mixture had cooled to room temperature, 1 M NaOH (10 mL) was added. The mixture was then extracted with ethyl acetate (10 mL). The organic phase was dried over Na_2SO_4 and filtered. The solvent was removed, and the residue was purified by silica gel chromatography using chloroform as a mobile phase to give 333 mg of **11a** (43.0%). ^{1}H NMR ($CDCl_3$) δ: 4.02 (s, broad, 2H), 4.30 (d, t, J_1 = 27.6 Hz, J_2 = 4.2 Hz, 2H), 4.79 (d, t, J_1 = 47.4 Hz, J_2 = 4.2 Hz, 2H), 6.68 (d, J = 8.7 Hz, 2H), 7.00 (d, J = 8.7 Hz, 2H), 7.36 (d, J = 15.3 Hz, 1H), 7.48 (d, J = 8.4 Hz, 2H), 7.75 (d, J = 15.3 Hz, 1H), 8.03 (d, J = 6.9 Hz, 2H). EI-MS: m/z 285 (M^+).

(*E*)-3-(4-Aminophenyl)-1-(4-(2-(fluoroethoxy)ethoxy)phenyl)-2-propen-1-one (11b). The reaction described above to prepare **11a** was used, and 85 mg of **11b** was obtained from **10b**. ^{1}H NMR ($CDCl_3$) δ: 3.77−3.94 (m, 4H), 4.00 (s, broad, 2H), 4.23 (t, J = 4.5 Hz, 2H), 4.53 (t, J = 4.2 Hz, 1H), 4.69 (t, J = 4.2 Hz, 1H), 6.68 (d, J = 8.4 Hz, 2H), 6.99 (d, J = 8.7 Hz, 2H), 7.74 (d, J = 15.6 Hz, 1H), 7.48 (d, J = 8.4 Hz, 1H), 7.36 (d, J = 15.3 Hz, 1H), 8.01 (d, J = 9.0 Hz, 2H). EI-MS: m/z 329 (M^+).

(*E*)-3-(4-Aminophenyl)-1-(4-(2-((fluoroethoxy)ethoxy)ethoxy)-phenyl)-2-propen-1-one (11c). The reaction described above to prepare **11a** was used, and 206 mg of **11c** was obtained from **10c**. ^{1}H NMR ($CDCl_3$) δ: 3.70−3.83 (m, 6H), 3.89 (t, J = 4.5 Hz, 2H), 4.12 (s, broad, 2H), 4.21 (t, J = 4.8 Hz, 2H), 4.49 (t, J = 4.0 Hz, 1H), 4.65 (t, J = 3.9 Hz, 1H), 6.67 (d, J = 8.7 Hz, 2H), 6.98 (d, J = 8.7 Hz, 2H), 7.36 (d, J = 15.3 Hz, 1H), 7.47 (d, J = 8.4 Hz, 2H), 7.74 (d, J = 15.9 Hz, 1H), 8.01 (d, J = 9.0 Hz, 2H). EI-MS: m/z 373 (M^+).

(*E*)-1-(4-(2-Fluoroethoxy)phenyl)-3-(4-(methylamino)phenyl)-2-propen-1-one (12a). To a solution of **11a** (290 mg, 1.02 mmol) in DMSO (6 mL) were added CH_3I (0.18 mL, 3.05 mmol) and anhydrous K_2CO_3 (691 mg, 5.08 mmol). The reaction mixture was stirred at room temperature for 3 h and poured into water. The mixture was extracted with ethyl acetate. The organic layers were combined and dried over Na_2SO_4. Evaporation of the solvent afforded a residue, which was purified by silica gel chromatography (hexane:ethyl acetate = 2:1) to give 90 mg of **12a** (29.5%). ^{1}H NMR ($CDCl_3$) δ: 2.89 (s, 3H), 4.23 (d, t, J_1 = 27.9 Hz, J_2 = 4.2 Hz, 2H), 4.79 (d, t, J_1 = 47.4 Hz, J_2 = 4.2 Hz, 2H), 6.59 (d, J = 8.7 Hz, 2H), 6.99 (d, J = 9.0 Hz, 2H), 7.34 (d, J = 15.3 Hz, 1H), 7.51 (d, J = 8.4 Hz, 2H), 7.78 (d, J = 15.3 Hz, 1H), 8.02 (d, J = 9.3 Hz, 2H). EI-MS: m/z 299 (M^+).

(*E*)-1-(4-(2-(Fluoroethoxy)ethoxy)phenyl)-3-(4-(methylamino)-phenyl)-2-propen-1-one (12b). The reaction described above to prepare **12a** was used, and 22 mg of **12b** was obtained from **11b**. ^{1}H NMR ($CDCl_3$) δ: 2.90 (s, 3H), 3.78−3.95 (m, 4H), 3.99 (s, broad, 1H), 4.23 (t, J = 4.5 Hz, 2H), 4.53 (t, J = 4.5 Hz, 2H), 4.53 (t, J = 4.2 Hz, 1H), 4.69 (t, J = 4.2 Hz, 1H), 6.60 (d, J = 8.7 Hz, 2H), 6.99 (d, J = 8.7 Hz, 2H), 7.35 (d, J = 15.3 Hz, 1H), 7.51 (d, J = 8.7 Hz, 2H), 7.77 (d, J = 15.3 Hz, 1H), 8.02 (d, J = 8.7 Hz, 2H). EI-MS: m/z 343 (M^+).

(*E*)-1-(4-(2-((Fluoroethoxy)ethoxy)ethoxy)phenyl)-3-(4-(methylamino)phenyl)-2-propen-1-one (12c). The reaction described above to prepare **12a** was used, and 53 mg of **12c** was obtained from **11c**. ^{1}H NMR ($CDCl_3$) δ: 2.89 (s, 3H), 3.69−3.83 (m, 6H), 3.90 (t, J = 4.8 Hz, 2H), 4.12 (s, broad, 1H), 4.22 (t, J = 5.1 Hz, 2H), 4.49 (t, J = 4.2 Hz, 1H), 4.65 (t, J = 4.1 Hz, 1H), 6.60 (d, J = 8.7 Hz, 2H), 6.98 (d, J = 9.0 Hz, 2H), 7.35 (d, J = 15.3 Hz, 1H), 7.51 (d, J = 8.7 Hz, 2H), 7.76 (d, J = 15.3 Hz, 1H), 8.01 (d, J = 8.7 Hz, 2H). EI-MS: m/z 387 (M^+).

(*E*)-3-(4-Dimethylaminophenyl)-1-(4-fluorophenyl)-2-propen-1-one (13). The reaction described above to prepare **5** was used, and 209 mg of **13** was obtained from 4-fluoroacetophenone and 4-dimethylbenzaldehyde. ^{1}H NMR (300 MHz, $CDCl_3$) δ: 3.03 (s, 6H), 6.68 (d, J = 8.7 Hz, 2H), 7.15 (t, J = 8.4 Hz, 2H), 7.30 (d, J = 15.3 Hz, 1H), 7.54 (d, J = 9.0 Hz, 2H), 7.78 (d, J = 15.3 Hz, 1H), 8.02−8.06 (m, 2H). EI-MS: m/z 269 (M^+).

(*E*)-1-(4-Fluorophenyl)-3-(4-nitrophenyl)-2-propen-1-one (14). The reaction described above to prepare **5** was used, and 490 mg of **14** was obtained from 4-fluoroacetophenone and 4-nitrobenzaldehyde. ^{1}H NMR (300 MHz, $CDCl_3$) δ: 7.21 (t, J = 8.7 Hz, 2H), 7.62 (d, J = 15.9 Hz, 1H), 7.80 (d, J = 8.7 Hz, 2H), 7.84 (d, J = 15.9 Hz, 1H), 8.07−8.12 (m, 2H), 8.29 (d, J = 8.7 Hz, 2H). EI-MS: m/z 271 (M^+).

(*E*)-3-(4-Aminophenyl)-1-(4-fluorophenyl)-2-propen-1-one (15). The reaction described above to prepare **11(a−c)** was used, and 150 mg of **15** was obtained from **14**. ^{1}H NMR (300 MHz, $CDCl_3$) δ: 4.07 (s, broad, 2H), 6.67 (d, J = 8.7 Hz, 2H), 7.15 (t, J = 8.7 Hz, 2H), 7.31 (d, J = 15.6 Hz, 1H), 7.47 (d, J = 8.4 Hz, 2H), 7.75 (d, J = 15.6 Hz, 1H), 8.03 (t, J = 8.7 Hz, 2H). EI-MS: m/z 241 (M^+).

(*E*)-1-(4-Fluorophenyl)-3-(4-methylaminophenyl)-2-propen-1-one (16). The reaction described above to prepare **12(a−c)** was used, and 14 mg of **16** was obtained from **15**. ^{1}H NMR (300 MHz, $CDCl_3$) δ: 2.90 (s, 3H), 4.20 (s, broad, 1H), 6.60 (d, J = 8.7 Hz, 2H), 7.17 (d, J = 8.7 Hz, 2H), 7.30 (d, J = 15.6 Hz, 1H), 7.50 (d, J = 8.7 Hz, 2H), 7.78 (d, J = 15.6 Hz, 1H), 8.04 (d, J = 8.7 Hz, 2H). EI-MS: m/z 255 (M^+).

(*E*)-2-(2-(2-(4-(3-(4-(Dimethylamino)phenyl)acryloyl)phenoxy)-ethoxy)ethoxy)ethyl 4-methylbenzenesulfonate (17). To a solution of **6c** (108 mg, 0.27 mmol) in pyridine (3 mL) was added tosyl chloride (343.8 mg, 0.621 mmol). The reaction mixture was stirred for 3 h at room temperature. After water was added, the mixture was extracted with ethyl acetate. The organic layer was dried over Na_2SO_4, and evaporation of the solvent afforded a residue, which was purified by preparative TLC (hexane:ethyl acetate = 1:1) to give 44 mg of **17** (29.4%). ^{1}H NMR (300 MHz, $CDCl_3$) δ: 2.43 (s, 3H), 3.04 (s, 6H), 3.62−3.72 (m, 6H),

3.85−3.87 (m, 2H), 4.15−4.18 (m, 4H), 6.70 (d, J = 8.7 Hz, 2H), 6.98 (d, J = 9.0 Hz, 2H), 7.31−7.35 (m, 2H), 7.37 (d, J = 9.0 Hz, 1H), 7.55 (d, J = 8.7 Hz, 2H), 7.80 (t, J = 8.7 Hz, 3H), 8.02 (d, J = 9.0 Hz, 2H). EI-MS m/z 553 (M^+)

Radiolabeling. Procedure for Labeling of 7a, 7b, 7c, and 13 with ^{11}C. ^{11}C was produced via a ^{14}N(p,α)^{11}C reaction with 16 MeV protons on a target of nitrogen gas with an ultracompact cyclotron (CYPRIS model 325R; Sumitomo Heavy Industry Ltd.) The $^{11}CO_2$ produced was transported to an automated system for the synthesis of ^{11}C-methyl iodide (CUPID C-100; Sumitomo Heavy Industry Ltd.) and converted sequentially to [^{11}C]MeOTf by the previously described method of Jewett.[33] [^{11}C]Chalcones were produced by reacting [^{11}C]MeOTf with the normethyl precursor, **7a**, **7b**, **7c**, and **13**, (0.5 mg) in 500 μL of methyl ethyl ketone (MEK). After the complete transfer of [^{11}C]MeOTf, ^{11}C-methylation was carried out for 5 min and the reaction solvent was then dried with a stream of nitrogen gas. The residue taken up in 200 μL of acetonitrile was purified by a reverse phase HPLC system (a Shimadzu LC-6A isocratic pump, a Shimadzu SPD-6A UV detector, and a Aloka NDW-351D scintillation detector) on a Cosmosil C_{18} column (Nakalai Tesque, 5C_{18}-AR-II, 10 mm × 250 mm) with an isocratic solvent of acetonitrile/water (55/45) at a flow rate of 6.0 mL/min. The desired fraction was collected in a flask and evaporated dry. The radiochemical yield, purity, and specific activity of [^{11}C]chalcones were further confirmed by analytical reverse phase HPLC on a 5C_{18}-AR-300 column (Nakalai Tesque, 4.6 mm × 150 mm, acetonitrile/water (60/40), 1.0 mL/min).

Procedure for Labeling 7c with ^{18}F. [^{18}F]Fluoride was produced by the JSW typeBC3015 cyclotron via an ^{18}O(p,n)^{18}F reaction and passed through a Sep-Pak Light QMA cartridge (Waters) as an aqueous solution in ^{18}O-enriched water. The cartridge was dried by airflow, and the ^{18}F activity was eluted with 0.5 mL of a Kryptofix 222/K_2CO_3 solution (11 mg of Kryptofix 222 and 2.6 mg of K_2CO_3 in acetonitrile/water (86/14)). The solvent was removed at 120 °C under a stream of argon gas. The residue was azeotropically dried with 1 mL of anhydrous acetonitrile twice at 120 °C under a stream of nitrogen gas and dissolved in DMSO (1 mL). A solution of tosylate precursor **17** (1.0 mg) in DMSO (1 mL) was added to the reaction vessel containing the ^{18}F activity in DMSO. The mixture was heated at 160 °C for 5 min. Water (5 mL) was added, and the mixture was passed through a preconditioned Oasis HLB cartridge (3 cm^3) (Waters). The cartridge was washed with 10 mL of water, and the labeled compound was eluted with 2 mL of acetonitrile. The eluted compound was purified by preparative HPLC [YMC-Pack Pro C_{18} column (20 mm × 150 mm), acetonitrile/water (75/25), flow rate 9.0 mL/min]. The retention time of the major byproduct of hydrolysis (t_R = 2.7 min) was well-resolved from the desired ^{18}F-labeled product (t_R = 10.7 min). The radiochemical purity and specific activity were determined by analytical HPLC [YMC-Pack Pro C_{18} column (4.6 mm × 150 mm), acetonitrile/water (60/40), flow rate 1.0 mL/min], and [^{18}F]**7c** was obtained in a radiochemical purity of > 99% with the specific activity of 35 GBq/mmol. Specific activity was estimated by comparing the UV peak intensity of the purified ^{18}F-labeled compound with a reference nonradioactive compound of known concentration.

Binding Assays Using the Aggregated Aβ peptides in Solution. Aβ(1−42) was purchased from Peptide Institute (Osaka, Japan). Aggregation was carried out by gently dissolving the peptide (0.25 mg/mL) in a buffer solution (pH 7.4) containing 10 mM sodium phosphate and 1 mM EDTA. The solution was incubated at 37 °C for 42 h with gentle and constant shaking. Binding experiments were carried out as described previously.[18] [^{125}I]DMIC with 2200 Ci/mmol of specific activity and radiochemical purity greater than 95% was prepared using the standard iododestannylation reaction. A mixture containing 50 μL of test compound (0.2 pM-400 μM in 10% EtOH), 50 μL of 0.02 nM [^{125}I]DMIC, 50 μL of Aβ(1−42) aggregates, and 850 μL of 10% EtOH was incubated at room temperature for 3 h. The mixture was then filtered through Whatman GF/B filters using a Brandel M-24 cell harvester, and the radioactivity of the filters containing the bound ^{125}I ligand was measured in a γ counter. Values for the half-maximal inhibitory concentration (IC_{50}) were determined from displacement curves of three independent experiments using GraphPad Prism 4.0, and those for the inhibition constant (K_i) were calculated using the Cheng−Prusoff equation: $K_i = IC_{50}/(1 + [L]/K_d)$, where [L] is the concentration of [^{125}I]DMIC used in the assay and K_d is the dissociation constant of DMIC (4.2 nM).[19] DMIC and IMPY used as test compounds for the inhibition assay were synthesized as reported previously.[19,34]

Biodistribution in Normal Mice. Experiments with animals were conducted in accordance with our institutional guidelines and approved by the Nagasaki University Animal Care Committee and the Kyoto University Animal Care Committee. A 100 μL amount of a saline solution containing the radiolabeled agent (3.7 MBq), EtOH (10%), and ascorbic acid (1 mg/mL) was injected directly into the tail vein of ddY mice (5-week-old, 22−25 g). Groups of five mice were sacrificed at various post-injection time points. The organs of interest were removed and weighed, and the radioactivity was measured with an automatic γ counter (COBRAII, Packard).

Staining of Aβ Plaques in Brain Sections of Tg2576 Transgenic Mice. The Tg2576 transgenic mice (female, 20-month-old) and wild-type (female, 20-month-old) mice were used as an Alzheimer's model and an age-matched control, respectively. After the mice were sacrificed by decapitation, the brains were immediately removed and frozen in powdered dry ice. The frozen blocks were sliced into serial sections 10 μm thick. Each slide was incubated with a 50% EtOH solution (100 μM) of compound **7c** for 10 min. The sections were washed with 50% EtOH for 3 min two times. After drying, the sections were then examined using a microscope (Nikon, Eclipse 80i) equipped with a B-2A filter set (excitation, 450−490 nm; diachronic mirror, 505 nm; long-pass filter, 520 nm). Thereafter, the serial sections were also immunostained with 3,3′-diaminobenzidine (DAB) as a chromogen using monoclonal antibodies against Aβ (amyloid β-protein immunohistostain kit, WAKO).

In Vitro Autoradiography Using Human AD Brains. Postmortem brain tissues from an autopsy-confirmed case of AD (73-year-old male) were obtained from BioChain Institute Inc. The presence and localization of plaques on the sections were confirmed with immunohistochemical staining using a monoclonal Aβ antibody as described above. The sections were incubated with [^{18}F]**7c** (54 μCi/200 μL) for 1 h at room temperature. They were then washed in 50% EtOH (two 1 min wash), before being rinsed with water for 30 s. After drying, the ^{18}F-labeled sections were exposed to a BAS imaging plate (Fuji Film, Tokyo, Japan) for 6 h. Ex vivo autoradiographic images were obtained using a BAS5000 scanner system (Fuji Film). After autoradiographic examination, the same sections were stained by thioflavin-S to confirm the presence of Aβ plaques. For the staining of thioflavin-S, sections were immersed in a 0.125% thioflavin-S solution containing 50% EtOH for 3 min and washed in 50% EtOH. After drying, the sections were then examined using a microscope (Nikon, Eclipse 80i) equipped with a B-2A filter set (excitation, 450−490 nm; diachronic mirror, 505 nm; long-pass filter, 520 nm).

Acknowledgment. This study was supported by the Program for Promotion of Fundamental Studies in Health Sciences of the National Institute of Biomedical Innovation (NIBIO), a Health Labour Sciences Research Grant, and a Grant-in-Aid for Young Scientists (A) and Exploratory Research from the Ministry of Education, Culture, Sports, Science and Technology, Japan.

Supporting Information Available: Representative HPLC chromatograms of [^{18}F]**7c**. This material is available free of charge via the Internet at http://pubs.acs.org.

References

(1) Hardy, J. A.; Higgins, G. A. Alzheimer's disease: the amyloid cascade hypothesis. *Science* **1992**, *256*, 184–185.
(2) Selkoe, D. J. Alzheimer's disease: genes, proteins, and therapy. *Physiol. Rev*. **2001**, *81*, 741–766.
(3) Nordberg, A. PET imaging of amyloid in Alzheimer's disease. *Lancet Neurol*. **2004**, *3*, 519–527.
(4) Mathis, C. A.; Wang, Y.; Klunk, W. E. Imaging β-amyloid plaques and neurofibrillary tangles in the aging human brain. *Curr. Pharm. Des*. **2004**, *10*, 1469–1492.
(5) Klunk, W. E.; Engler, H.; Nordberg, A.; Wang, Y.; Blomqvist, G.; Holt, D. P.; Bergstrom, M.; Savitcheva, I.; Huang, G. F.; Estrada, S.; Ausen, B.; Debnath, M. L.; Barletta, J.; Price, J. C.; Sandell, J.; Lopresti, B. J.; Wall, A.; Koivisto, P.; Antoni, G.; Mathis, C. A.; Langstrom, B. Imaging brain amyloid in Alzheimer's disease with Pittsburgh Compound-B. *Ann. Neurol*. **2004**, *55*, 306–319.
(6) Mathis, C. A.; Wang, Y.; Holt, D. P.; Huang, G. F.; Debnath, M. L.; Klunk, W. E. Synthesis and evaluation of ^{11}C-labeled 6-substituted 2-arylbenzothiazoles as amyloid imaging agents. *J. Med. Chem*. **2003**, *46*, 2740–2754.
(7) Verhoeff, N. P.; Wilson, A. A.; Takeshita, S.; Trop, L.; Hussey, D.; Singh, K.; Kung, H. F.; Kung, M. P.; Houle, S. In vivo imaging of Alzheimer disease β-amyloid with [^{11}C]SB-13 PET. *Am. J. Geriatr. Psychiatry* **2004**, *12*, 584–595.
(8) Ono, M.; Wilson, A.; Nobrega, J.; Westaway, D.; Verhoeff, P.; Zhuang, Z. P.; Kung, M. P.; Kung, H. F. ^{11}C-Labeled stilbene derivatives as Abeta-aggregate-specific PET imaging agents for Alzheimer's disease. *Nucl. Med. Biol*. **2003**, *30*, 565–571.
(9) Small, G. W.; Kepe, V.; Ercoli, L. M.; Siddarth, P.; Bookheimer, S. Y.; Miller, K. J.; Lavretsky, H.; Burggren, A. C.; Cole, G. M.; Vinters, H. V.; Thompson, P. M.; Huang, S. C.; Satyamurthy, N.; Phelps, M. E.; Barrio, J. R. PET of brain amyloid and tau in mild cognitive impairment. *N. Engl. J. Med*. **2006**, *355*, 2652–2663.
(10) Shoghi-Jadid, K.; Small, G. W.; Agdeppa, E. D.; Kepe, V.; Ercoli, L. M.; Siddarth, P.; Read, S.; Satyamurthy, N.; Petric, A.; Huang, S. C.; Barrio, J. R. Localization of neurofibrillary tangles and β-amyloid plaques in the brains of living patients with Alzheimer disease. *Am. J. Geriatr. Psychiatry* **2002**, *10*, 24–35.
(11) Rowe, C. C.; Ackerman, U.; Browne, W.; Mulligan, R.; Pike, K. L.; O'Keefe, G.; Tochon-Danguy, H.; Chan, G.; Berlangieri, S. U.; Jones, G.; Dickinson-Rowe, K. L.; Kung, H. P.; Zhang, W.; Kung, M. P.; Skovronsky, D.; Dyrks, T.; Holl, G.; Krause, S.; Friebe, M.; Lehman, L.; Lindemann, S.; Dinkelborg, L. M.; Masters, C. L.; Villemagne, V. L. Imaging of amyloid β in Alzheimer's disease with ^{18}F-BAY94-9172, a novel PET tracer: proof of mechanism. *Lancet Neurol*. **2008**, *7*, 129–135.
(12) Zhang, W.; Oya, S.; Kung, M. P.; Hou, C.; Maier, D. L.; Kung, H. F. F-18 polyethyleneglycol stilbenes as PET imaging agents targeting Aβ aggregates in the brain. *Nucl. Med. Biol*. **2005**, *32*, 799–809.
(13) Lockhart, A. Imaging Alzheimer's disease pathology: one target, many ligands. *Drug Discovery Today* **2006**, *11*, 1093–1099.
(14) Ye, L.; Morgenstern, J. L.; Gee, A. D.; Hong, G.; Brown, J.; Lockhart, A. Delineation of positron emission tomography imaging agent binding sites on β-amyloid peptide fibrils. *J. Biol. Chem*. **2005**, *280*, 23599–235604.
(15) Lockhart, A.; Ye, L.; Judd, D. B.; Merritt, A. T.; Lowe, P. N.; Morgenstern, J. L.; Hong, G.; Gee, A. D.; Brown, J. Evidence for the presence of three distinct binding sites for the thioflavin T class of Alzheimer's disease PET imaging agents on β-amyloid peptide fibrils. *J. Biol. Chem*. **2005**, *280*, 7677–7684.
(16) Ono, M.; Yoshida, N.; Ishibashi, K.; Haratake, M.; Arano, Y.; Mori, H.; Nakayama, M. Radioiodinated flavones for in vivo imaging of β-amyloid plaques in the brain. *J. Med. Chem*. **2005**, *48*, 7253–7260.
(17) Ono, M.; Watanabe, R.; Kawashima, H.; Kawai, T.; Watanabe, H.; Haratake, M.; Saji, H.; Nakayama, M. ^{18}F-Labeled flavones for in vivo imaging of β-amyloid plaques in Alzheimer's brains. *Bioorg. Med. Chem*. **2009**, *17*, 2069–2076.
(18) Ono, M.; Hori, M.; Haratake, M.; Tomiyama, T.; Mori, H.; Nakayama, M. Structure−activity relationship of chalcones and related derivatives as ligands for detecting of β-amyloid plaques in the brain. *Bioorg. Med. Chem*. **2007**, *15*, 6388–6396.
(19) Ono, M.; Haratake, M.; Mori, H.; Nakayama, M. Novel chalcones as probes for in vivo imaging of β-amyloid plaques in Alzheimer's brains. *Bioorg. Med. Chem*. **2007**, *15*, 6802–6809.
(20) Maya, Y.; Ono, M.; Watanabe, H.; Haratake, M.; Saji, H.; Nakayama, M. Novel radioiodinated aurones as probes for SPECT imaging of β-amyloid plaques in the brain. *Bioconjugate Chem*. **2009**, *20*, 95–101.
(21) Ono, M.; Maya, Y.; Haratake, M.; Ito, K.; Mori, H.; Nakayama, M. Aurones serve as probes of β-amyloid plaques in Alzheimer's disease. *Biochem. Biophys. Res. Commun*. **2007**, *361*, 116–121.
(22) Stephenson, K. A.; Chandra, R.; Zhuang, Z. P.; Hou, C.; Oya, S.; Kung, M. P.; Kung, H. F. Fluoro-pegylated (FPEG) imaging agents targeting Aβ aggregates. *Bioconjugate Chem*. **2007**, *18*, 238–246.
(23) Qu, W.; Kung, M. P.; Hou, C.; Oya, S.; Kung, H. F. Quick assembly of 1,4-diphenyltriazoles as probes targeting β-amyloid aggregates in Alzheimer's disease. *J. Med. Chem*. **2007**, *50*, 3380–3387.
(24) Zhang, W.; Oya, S.; Kung, M. P.; Hou, C.; Maier, D. L.; Kung, H. F. F-18 stilbenes as PET imaging agents for detecting β-amyloid plaques in the brain. *J. Med. Chem*. **2005**, *48*, 5980–5988.
(25) Kung, M. P.; Hou, C.; Zhuang, Z. P.; Zhang, B.; Skovronsky, D.; Trojanowski, J. Q.; Lee, V. M.; Kung, H. F. IMPY: an improved thioflavin-T derivative for in vivo labeling of β-amyloid plaques. *Brain Res*. **2002**, *956*, 202–210.
(26) Hsiao, K.; Chapman, P.; Nilsen, S.; Eckman, C.; Harigaya, Y.; Younkin, S.; Yang, F.; Cole, G. Correlative memory deficits, Aβ elevation, and amyloid plaques in transgenic mice. *Science* **1996**, *274*, 99–102.
(27) Kuntner, C.; Kesner, A. L.; Bauer, M.; Kremslehner, R.; Wanek, T.; Mandler, M.; Karch, R.; Stanek, J.; Wolf, T.; Muller, M.; Langer, O. Limitations of small animal PET imaging with [^{18}F]FDDNP and FDG for quantitative studies in a transgenic mouse model of Alzheimer's disease. *Mol. Imaging Biol*. **2009**, *11*, 236–240.
(28) Klunk, W. E.; Lopresti, B. J.; Ikonomovic, M. D.; Lefterov, I. M.; Koldamova, R. P.; Abrahamson, E. E.; Debnath, M. L.; Holt, D. P.; Huang, G. F.; Shao, L.; DeKosky, S. T.; Price, J. C.; Mathis, C. A. Binding of the positron emission tomography tracer Pittsburgh compound-B reflects the amount of amyloid-β in Alzheimer's disease brain but not in transgenic mouse brain. *J. Neurosci*. **2005**, *25*, 10598–10606.
(29) Maeda, J.; Ji, B.; Irie, T.; Tomiyama, T.; Maruyama, M.; Okauchi, T.; Staufenbiel, M.; Iwata, N.; Ono, M.; Saido, T. C.; Suzuki, K.; Mori, H.; Higuchi, M.; Suhara, T. Longitudinal, quantitative assessment of amyloid, neuroinflammation, and anti-amyloid treatment in a living mouse model of Alzheimer's disease enabled by positron emission tomography. *J. Neurosci*. **2007**, *27*, 10957–10968.
(30) Toyama, H.; Ye, D.; Ichise, M.; Liow, J. S.; Cai, L.; Jacobowitz, D.; Musachio, J. L.; Hong, J.; Crescenzo, M.; Tipre, D.; Lu, J. Q.; Zoghbi, S.; Vines, D. C.; Seidel, J.; Katada, K.; Green, M. V.; Pike, V. W.; Cohen, R. M.; Innis, R. B. PET imaging of brain with the β-amyloid probe, [^{11}C]6-OH-BTA-1, in a transgenic mouse model of Alzheimer's disease. *Eur. J. Nucl. Med. Mol. Imaging* **2005**, *32*, 593–600.
(31) Skovronsky, D. M.; Zhang, B.; Kung, M. P.; Kung, H. F.; Trojanowski, J. Q.; Lee, V. M. In vivo detection of amyloid plaques in a mouse model of Alzheimer's disease. *Proc. Natl. Acad. Sci. U.S.A* **2000**, *97*, 7609–7614.
(32) Saido, T. C.; Iwatsubo, T.; Mann, D. M.; Shimada, H.; Ihara, Y.; Kawashima, S. Dominant and differential deposition of distinct β-amyloid peptide species, A β N3(pE), in senile plaques. *Neuron* **1995**, *14*, 457–466.
(33) Jewett, D. M. A simple synthesis of [^{11}C]methyl triflate. *Int. J. Radiat. Appl. Instrum. A* **1992**, *43*, 1383–1385.
(34) Zhuang, Z. P.; Kung, M. P.; Wilson, A.; Lee, C. W.; Plossl, K.; Hou, C.; Holtzman, D. M.; Kung, H. F. Structure−activity relationship of imidazo[1,2-*a*]pyridines as ligands for detecting β-amyloid plaques in the brain. *J. Med. Chem*. **2003**, *46*, 237–243.